Available online at BCREC website: https://bcrec.id

Bulletin of Chemical Reaction Engineering & Catalysis, 17 (4) 2022, 712-724

Research Article

Highly Selective Bio-hydrocarbon Production using Sidoarjo Mud Based-Catalysts in the Hydrocracking of Waste Palm Cooking Oil

Wega Trisunaryanti*, T. Triyono, Iip Izul Fallah, Shafira Salsiah, Gesha Desy Alisha

Department of Chemistry, Faculty of Mathematics and Natural Sciences, Universitas Gadjah Mada, Yogyakarta 55281, Indonesia.

Received: 12nd August 2022; Revised: 28th September 2022; Accepted: 29th September 2022
Available online: 1st October 2022; Published regularly: December 2022

Abstract

In this work, Lapindo mud (LM) was used as catalyst support. This is because the Lapindo mud has a high SiO_2 content of 45.33 %. This research aims to produce a hydrocracking catalyst based on Lapindo mud through impregnation of Ni and Pt metals as well as grafting amine groups. Ni and Pt metals impregnation using wet impregnation method followed by amine group grafting. The best catalyst in this study was NiPt-NH_2/LM which contained Ni and Pt metals, surface area, and pore diameters of 1.68 wt.% and 0.4 wt.%, 6.59 m^2/g, 15.51 nm, respectively. The effectiveness of the catalyst was tested against temperature and catalyst: feed ratio. The catalyst with the best activity and selectivity was tested for reusability 3 times through hydrocracking process. The yield of liquid products obtained in the hydrocracking process of WPO using NiPt-NH_2/LM catalyst with the optimum temperature and the weight ratio of catalyst:feed at 550 ^oC was 79.4 wt. % which consists of hydrocarbon compound of 55.9 wt.%. The yield of liquid products obtained in the hydrocracking WPO using the used NiPt-BH_2/LM catalyst was 28.4 wt.% which consists of hydrocarbon compound of 23.6 wt.%.

Copyright © 2022 by Authors, Published by BCREC Group. This is an open access article under the CC BY-SA License (https://creativecommons.org/licenses/by-sa/4.0).

Keywords: Bimetallic Ni-Pt; Hydrocracking; ammonia-functionalized catalyst; Mud catalyst; Reusable catalyst

How to Cite: Trisunaryanti, W., Triyono, T., Fallah, I.I., Salsiah, S., Alisha, G.D. (2022). Highly Selective Bio-hydrocarbon Production using Sidoarjo Mud Based-Catalysts in the Hydrocracking of Waste Palm Cooking Oil. *Bulletin of Chemical Reaction Engineering & Catalysis*, 17(4), 712-724 (doi: 10.9767/bcrec.17.4.15472.712-724)

Permalink/DOI: https://doi.org/10.9767/bcrec.17.4.15472.712-724

1. Introduction

The increasing population growth can affect energy needs, which generally use fossil fuels as an energy source. Where fossil fuels are non-renewable energy sources [1]. Biofuel or liquid biofuel is a renewable energy source that can replace fossil fuels. Biofuels or liquid biofuels can be obtained from various types of biomass, which are promising as a substitute for fossil fuels used in transportation, heating services, and power generation [2].

One of the materials that can be converted into biofuel is waste cooking oil [3-5]. The use of waste cooking oil (WCO) continues to increase and there is no further handling of waste cook-

* Corresponding Author.
Email: wegats@ugm.ac.id (W. Trisunaryanti)

ing oil. This is one of the causes of environmental pollution that continues to increase [6]. In addition, the main component of waste cooking oil is triglycerides which can be easily converted into biofuels [7,8]. However, the high oxygen content in triglycerides causes the final product to contain oxygen such as FAME. This can lead to poor storage stability, low mixing rates with petroleum diesel and cause engine compatibility issues [9]. These disadvantages of biofuel production can be overcome using hydrocracking techniques [10]. Cracking is divided into two, namely thermal cracking and catalytic cracking [11]. The use of catalytic cracking is better than thermal cracking because it produces liquid products and hydrocarbon compounds of a quite high [12-14]. In catalytic cracking process, a catalyst is needed. The catalyst commonly used is a metal catalyst impregnated in the support [15,16]. The presence of metal catalyst in hydrocracking process is gaining interest due to its facile separation and a promising candidate for deoxygenation reactions [17]. Catalyst has the main function to provide hydrogenation reaction to produce a high liquid hydrocarbon yield and restrain coke formation [18]. The use of metal catalysts in the cracking process requires support. The support is the use of Lapindo Mud (LM). This is because the Lapindo Mud (LM) has various metal oxides that can be used as heterogeneous catalyst and also supports [19]. The content of silica within Lapindo Mud can reach about 55%. Moreover, Lapindo Mud (LM) contains metal oxides, such as SiO_2 and Al_2O_3 [20]. In addition, this research uses the amine group, where the amine group acts a mesoporous support which is useful for capturing FFA [21]. According to Kandel [22], with the use of Ni-NH_2/LM in capturing FFA managed to capture 47% by weight and convert 66% by weight into liquid hydrocarbons.

Based on the background, hydrotreatment of waste palm oil (WPO) was done in the presence of monometallic Ni, Pt, and bimetallic NiPt supported on amine-functionalized Lapindo Mud. The combination of two modifications is expected to improve the activity and selectivity of bimetallic NiPt-NH_2/LM on its performance. The performance of each catalyst are compared from the product conversion and liquid hydrocarbons produced during hydrotreatment process. Furthermore, the hydrocracking effects, such as the variation of temperature and catalyst:feed ratio and the reusability, were tested.

2. Materials and Methods

2.1 Materials

Lapindo mud was obtained from Sidoarjo, East Java, Indonesia. Metal precursors nickel(II) chloride hexahydrate ($NiCl{\cdot}6H_2O$), metal precursors platinum(IV) chloride ($PtCl_4$), 3-aminopropyl trimethoxysilane (3-APTMS), toluene (99.9%) and methanol (99.9%) were purchased from Tokyo Chemical Industry Co. Waste palm oil obtained collectively from domestic waste to be used as feed in the hydrocracking process.

2.2 Sample Preparation

The LM was crushed with 100 mesh sieve to obtained fine particles. The impregnation method was done through wet impregnation. Three variations of metal were synthesized Ni/LM, Pt/LM, and NiPt/LM. The monometallic Ni/LM and Pt/LM were synthesized in 2 g of LM under constant stirring at 300 rpm in an aqueous solution at room temperature. Whereas, the bimetallic NiPt/LM was synthesized using co-impregnation method, by comparison metal of Ni and Pt 1:0.05 in 2 g of LM under constant stirring at 300 rpm in an aqueous solution at room temperature. After mixing, the materials water was removed from the mixture at 80 ^oC. The materials were calcined at 500 ^oC with a heating rate 5 ^oC/min for 3 h under flow N_2 (20 mL/min), followed by reduction at 450 ^oC with heating rate 5 ^oC/min for 3 h with under ambient pressure.

Amine-functionalized catalysts were prepared by grafting method of 3-APTMS (1 mmol, 0.18 g, 174 µL) to the surface of each LM supported metal catalyst in 20 mL of refluxed toluene under constant stirring for 6 h at 90 ^oC. The grafted catalysts were centrifuged at 2000 rpm for 2 min, then washed several times by using methanol to remove any excess APTMS. After removal, water was removed from the mixture at 80 ^oC.

2.3 Catalytic Activity Test

All catalysts materials were evaluated in the hydrocracking of waste palm oil using a semi-batch reactor system for 2 h under an H_2 gas flow rate 20 mL/min with under ambient pressure. A semi-batch reactor system is a reactor in which some reactants are added to the reactor at the start of the batch, while others are fed intermittently or continuously during of the reaction [23]. The hydrocracking process was done at various temperatures of 500; 550;

Copyright © 2022, ISSN 1978-2993

600 °C, with catalyst:feed ratios of 1:50, 1:100, and 1:200 (w/w) as well as the reusability test of the best catalyst for the waste palm oil conversion. The liquid products were analyzed using GC-MS. The results of yield and conversion were calculated using the equations below:

$$Liquid\ Product\ Yield\ (\%) = \frac{W_{LP}}{W_{WPO}} x100\% \quad (1)$$

$$Residue\ Yield\ (\%) = \frac{W_R}{W_{WPO}} x100\% \quad (2)$$

$$Coke\ Yield\ (\%) = \frac{W_C}{W_{WPO}} x100\% \quad (3)$$

$$Gas\ Yield\ (\%) = \frac{W_{WPO} - W_L - W_C}{W_{WPO}} x100\% \quad (4)$$

$$Total\ Conversion\ (\%) = \frac{W_{WPO} - W_R}{W_{WPO}} x100\% \quad (5)$$

where, W_{LP} is the weight of the liquid product (g), W_{WPO} is the weight of waste palm cooking oil (g), W_R is the weight of the remaining oil (g), and W_C is the weight of the coke (g).

2.4 Sample Characterization

The functional groups constructing all catalyst were recorded between 4000 to 400 cm^{-1} using Fourier transform infrared spectrometer (FTIR, Shimadzu Prestige 21) with KBr disc technique. The crystallinity of catalyst was characterized using X-ray Diffraction (XRD, Bruker D2 Phaser 2nd Gen). The surface area of all catalyst materials were analyzed using surface area analyzer gas sorption Quantachrome NovaWin2 1200e version 2.2. The chemical composition in LM was analyzed using X-ray Fluorescence (XRF, RIGAKU-NEX QC+QuanTEZ) with detector <160 eV @Mn K-Alpha line. The pore images of catalysts were captured by using TEM (JEOL-JEM-1400) at 120 kV. The liquid products produced from each hydrocracking of waste palm oil were analyzed for the content hydrocarbons and other compounds produced using gas chromatography-mass spectrometry (GC-MS, Shimadzu QP2010) with pyrolysis method, type of column of HP-5 GC, and carrier gas of Helium.

3. Results and Discussion

3.1 Quantitative Analysis of Lapindo Mud

It can be seen in Table 1 that the Lapindo mud consists of various types of metal oxides, especially SiO_2 (45.33 %), Fe_2O_3 (24.24 %) and Al_2O_3 (18.83 %) which in previous studies acted as a constituent of hydrocracking catalyst [13,24,25]. The data confirm that Lapindo mud can be used as a support and hydrocracking catalyst.

3.2 Characterizations of Catalyst

3.2.1 Characterization of LM support

In this study, LM is used as a support. The LM was calcined in order to remove impurities that can interfere with the catalyst performance. LM functional groups were characterized using FTIR shown in Figure 1. Around 470, 779, and 1033 cm^{-1} are a signal for Si–O–Si bending vibration [26,27]. Around 1427 cm^{-1} is an indication of the stretching vibration of Si–O–Al [28]. Around 1635 cm^{-1} is a signal scissor-bending vibrations of water molecules. While, peak around 3425 cm^{-1} for bending O–H originating from water molecules and 3626 cm^{-1} which is the OH stretching vibration of aluminol (Al-OH) [19,29].

Figure 2 presents a XRD characterization of LM before and after calcination. LM majority have crystalline structure displayed at 2θ around 20° to 30° which indicate a characteristic for amorphous silica-alumina [30]. The dif-

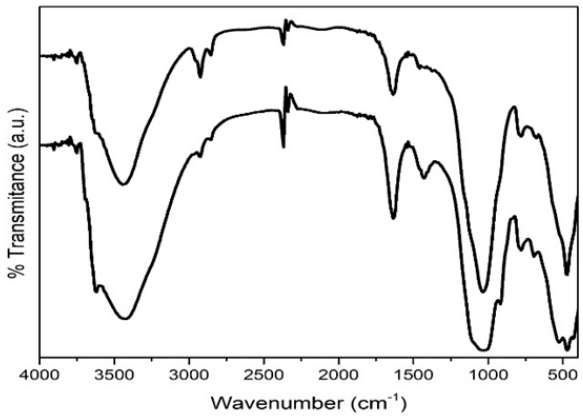

Figure 1. FTIR spectra of LM (a) before and (b) after calcination

Table 1. XRF analysis of Lapindo Mud (LM)

Meta oxides	Composition (%)
Al_2O_3	18.83
SiO_2	45.33
K_2O	1.27
CaO	2.02
TiO_2	0.75
MnO	0.15
Fe_2O_3	24.24
ClO	7.40

Copyright © 2022, ISSN 1978-2993

fractogram has a high peak at 2θ = 26.5° which indicates amorphous SiO_2 (ICDD 01-083-2187) [31]. In addition, the sample presents characteristic low-intensities peaks approximately 37° and 68° indicating Al_2O_3 [32]. On the diffractogram around 20°-40°, it can be observed that LM after calcination has a shorter peak than before calcination. This is due to the effect of calcination at high temperatures which causes evaporation of volatile compounds and the formation of oxide compounds [33,34].

3.2.2 Characterizations of catalysts

LM was impregnated with two metals, namely Ni and Pt metal through the wet impregnation method. Table 2 shows that the impregnation of Ni and Pt metals was successful. Ni metal has a smaller size than Pt metal so that Ni metal can enter more LM pores [35,36].

The success of the impregnation of Ni and Pt metals is also supported by XRD data. The XRD analysis shown in Figure 3 revealed that all catalyst with Ni exhibit sharp peaks positioned at 37.3° and 62.7°, indexed as (204), and (220) (ICDD card no. 01-078-0145), and Pt particles have a diffraction peak at 38.4°, 50.3°, and 68.4°, indexed as (410), (431), and (442) (ICDD no. 00-039-0411). This indicates that the peaks are the characteristics peaks of NiO and PtO_x, respectively [37,38]. The broad weak peaks indicate that Ni metal is amorphous which may be due to its small size and its high dispersion [39]. The high dispersion prevents the metal from forming agglomeration and crystallization, thereby explaining the appearance of the amorphous signal [40].

Pore analysis is determined by BET and BJH calculation in Table 2, in which LM has a

Table 2. Bulk characterizations of catalysts

Catalyst	Surface Area ($m^2.g^{-1}$)[a]	Pore Volume ($cm^3.g^{-1}$)[a]	Pore Diameter (nm)[a]	Metal loading (wt%)[b]	
				Ni	Pt
LM	5.67	0.0574	27.12	-	-
Ni/LM	10.33	0.0610	15.72	6.48	-
Pt/LM	9.61	0.0043	13.17	-	0.86
NiPt/LM	10.45	0.0594	14.62	8.86	0.10
NH_2/LM	1.03	0.0209	14.18	-	-
Ni-NH_2/LM	6.7	0.0451	19.66	5.53	-
Pt-NH_2/LM	3.64	0.0184	8.85	-	0.3
NiPt-NH-$_2$/LM	6.59	0.0450	15.51	1.68	0.04

[a] Surface area, pore volume and pore diameter is calculated by BET and BJH
[b] Metal composition is quantitatively determined by X-ray Fluorescence

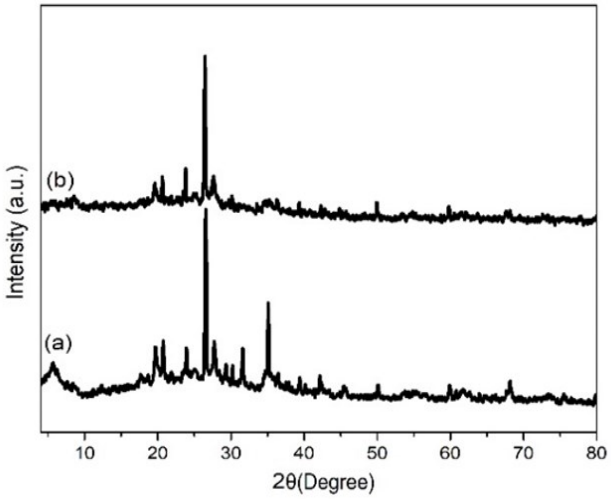

Figure 2. The diffractogram of (a) LM before calcination and (b) LM after calcination

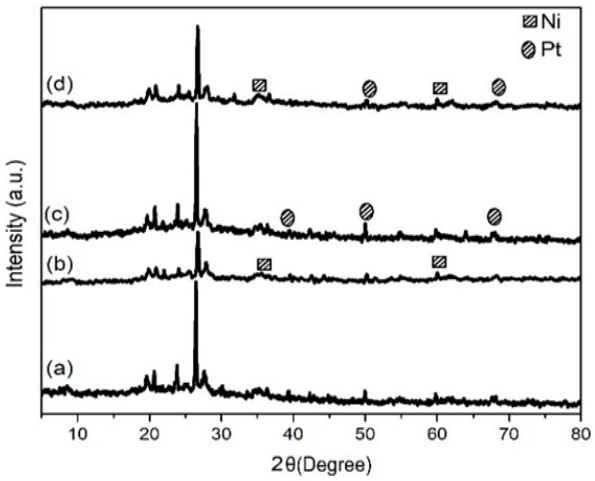

Figure 3. The diffractogram of (a) LM, (b) Ni/LM, (c) Pt/LM, and (d) NiPt/LM

Copyright © 2022, ISSN 1978-2993

pore diameter of 5.67 nm which indicates the category of mesoporous material. Meanwhile, the pore size distribution graph can be seen in Figure 4 which shows that the Ni and Pt metals are evenly distributed in the pore materials. However, in the pore distribution, Pt metal only blocked some pores. This can be attributed to drastic decrease in pore volume. Moreover, the decrease in pore volume and pore diameter is due to blockage of the catalyst pores by Ni and Pt metals.

In the next step, all catalysts were modified by adding an amine group. This is done to increase the catalytic activity in the hydrocracking process of waste palm cooking oil [41]. Characterization using FTIR was carried out to determine the addition of the amine group shown in Figure 5. The amine group grafting was successful where it can be seen in Figure 5 that there is a peak at 1558 cm^{-1} and 3400 cm^{-1}. This peak respectively indicates the bending and stretching of N–H bond in the structure APTMS. In addition, the success of the amine functionalization was also shown by the presence of an anti-symmetrical stretching band of –(–CH_2) at 2931 cm^{-1} and the weakening vibra-

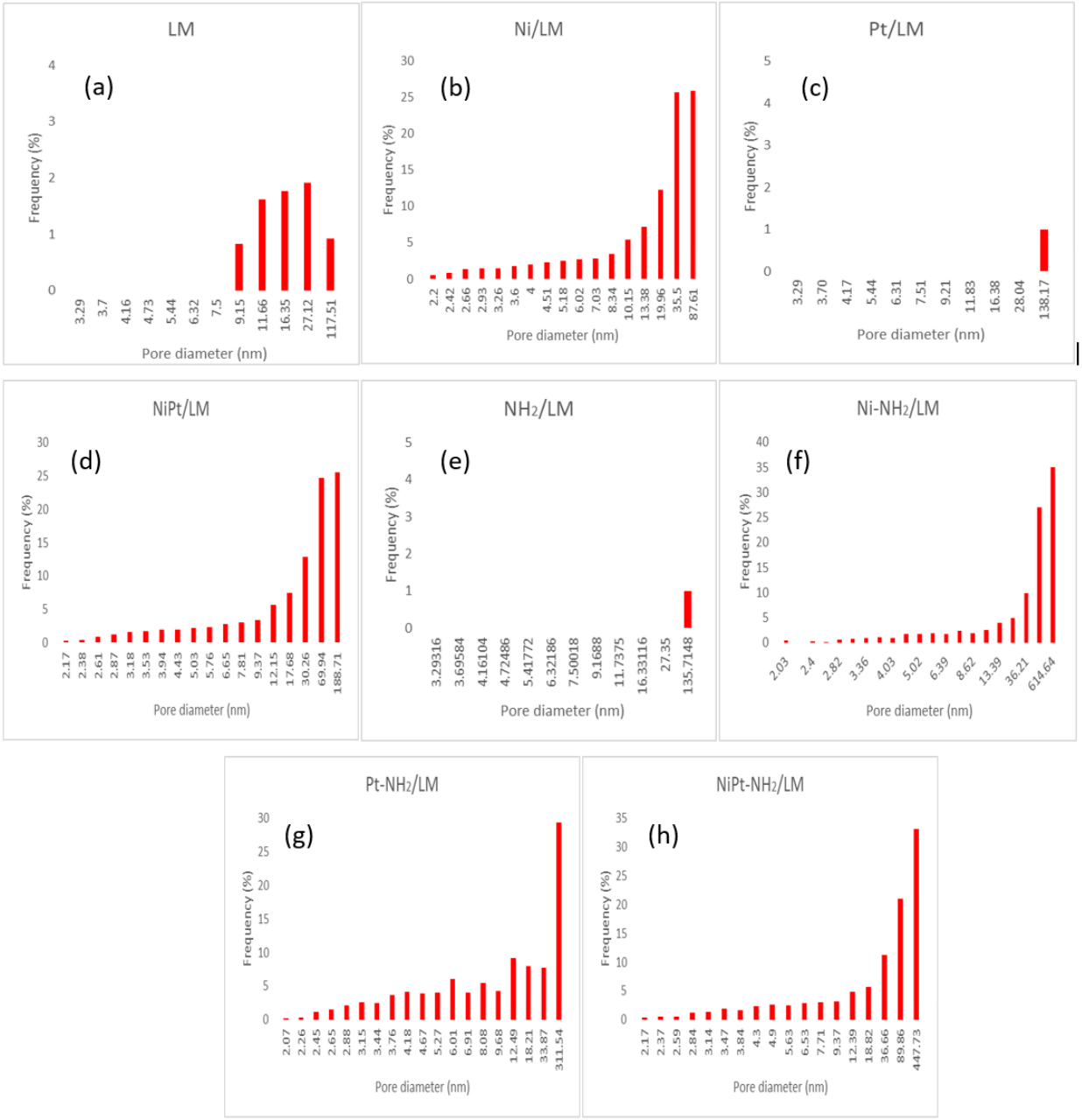

Figure 4. Pore size distribution graph of (a) LM, (b) Ni/LM, (c) Pt/LM, (d) NiPt/LM, (e) NH_2/LM, (f) Ni-NH_2/LM, (g) Pt-NH_2/LM (h) NiPt-NH-$_2$/LM

Copyright © 2022, ISSN 1978-2993

tion of Si–OH at 956 cm^{-1} after the addition of the amine which indicated the replacement of the silanol group with Si–O–Si in the condensation reaction during the functionalization process [26].

The amino-propyl functional group has a longer chain than the silanol group initially present on the surface of the LM support, which in turn fills more space in the silica pore. Therefore, the addition of new functional groups is expected to cause a decrease in surface area, pore diameter, and pore volume on the catalyst because it is expected that less N_2 gas can access the pores during the gas adsorption analysis (Table 1). However, the Ni-NH_2/LM and NiPt-NH_2/LM catalysts have larger pore diameters. This is caused by the amine group that does not block the catalyst pores completely.

3.3 Catalytic Activity of Catalyst

Catalytic activity test was carried out on all catalysts, while as a comparison, thermal hydrocracking (without catalyst) was also carried out. The hydrocracking process WPO were done at 550 ^oC under the flow of H_2 gas for 2 h. The utilization of heterogeneous catalyst is used to convert oxygenated compounds of waste palm oil into short-chain carbon [42]. The conversion and product distribution from the hydrocracking process of WPO with a feed ratio of 1:50 is summarized in Table 3.

The results of thermal cracking products represented a fairly high amount of liquid product (61.4 wt.%), which contained a total of 25.5 wt.% hydrocarbon compounds and 36 wt.% oxygenated compounds. The high level of oxygenated compounds makes the liquid product unsuitable for use as a fuel. By comparing thermal hydrocracking and hydrocracking using LM catalysts, there has been an increase in the gaseous product. This is due to the breakdown of long-chain hydrocarbons into short-chain hydrocarbons [43].

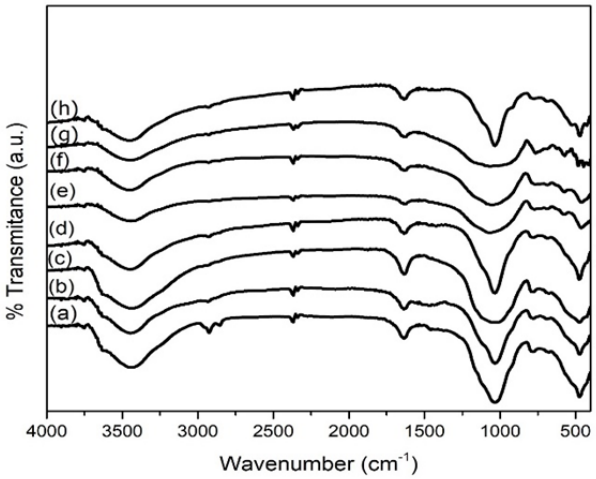

Figure 5. FTIR spectra of (a) LM, (b) NH_2/LM, (c) Ni/LM, (d) Ni-NH_2/LM, (e) Pt/LM, (f) Pt-NH_2/LM, (g) NiPt/LM, (h) NiPt-NH_2-/LM.

Table 3. Product conversion and liquid fraction from hydrocracking of WPO

Hydro-cracking conditions	Total Conversion (wt.%)	Product distribution (wt.%)						
		Gas Product	Liquid Product					Coke*
			C_5-C_{12}	C_{13}-C_{20}	Total hydrocarbons	Oxygenates	Others	
Thermal	99.7	38.2	13.8	11.7	25.5	16.2	19.8	*nd*
LM	99.4	43.2	2.6	8.3	10.9	29.3	16	0.6
Ni/LM	99.7	57.3	12.8	19.5	32.3	9.3	0.8	0.3
Pt/LM	99.7	63.4	15.7	14.6	30.3	2.1	3.9	0.3
NiPt/LM	99.8	34.8	12.1	24.8	36.9	9.0	19.1	0.2
NH_2/LM	99.5	30.2	26.5	25.0	51.5	6.0	11.8	0.5
Ni-NH_2/LM	99.6	37.4	29.9	24.4	54.3	3.6	4.3	0.4
Pt-NH_2/LM	99.7	52.3	24.0	20.4	44.4	1.1	1.9	0.3
NiPt-NH_2/LM	99.7	20.4	27.4	28.5	55.9	6.8	16.6	0.3

*Coke is waste palm oil that is deposited on the surface of the catalyst which cannot be converted into biofuel
nd: not detected

Copyright © 2022, ISSN 1978-2993

As a catalyst, LM has a high amount SiO_2 which is known to increase the acid content surface [44]. The acidity material affected the formation of carbenium ions by initiation on acid site, hence producing more short-chain hydrocarbons [30,45]. LM which contains high metal oxides can support the deoxygenation reaction to form long chain hydrocarbons. LM has a lower total of hydrocarbon compounds compared to thermal conditions due to too many products that are converted to gaseous products and the resulting liquid product produce oxygenate compounds which are quite high as well.

The increase in the catalytic activity of the catalyst was carried out by the impregnation of monometallic and bimetallic metals. In this study, Ni and Pt monometallic as well as NiPt bimetallic metals were used. As expected, the impregnation of Ni and Pt metals increased the catalytic activity. This is because Ni has two unpaired electrons in its *d* orbital which are active in the dissociation of H_2 during hydrocracking process, whereas Pt as a noble metal is known to be the best catalyst for hydrocarbon reforming and alcohol because of its remarkable ability to break C–C bonds [26,46]. In addition, bimetallic metal impregnation on LM support was done, on the grounds that bimetallic catalysts using Pt and *3d* metals (Ni) have shown better activity than monometallic Pt in deoxygenation mechanism [47]. Modification of the bimetallic catalyst increased the liquid product and hydrocarbon compounds by 65.6 wt.% and 36.9 wt.% respectively, which is higher than the liquid product and hydrocarbon compounds produced by monometallic catalysts (Ni/LM and Pt/LM) (Table 3).

WPO is converted into biofuel, where WPO contains triglycerides and free fatty acids (FFA), triglycerides are converted to hydrocarbons through a dehydrogenation mechanism. The deoxygenation mechanism consists of three reactions namely decarboxylation, decarbonylation, and hydrodeoxygenation [48]. LM, Ni/LM, Pt/LM, and NiPt/LM catalysts are included in the decarboxylation, and decarbonylation mechanism processes. This is because the cracking process using the catalyst produces a high enough gas (Table 3). This shows that there is a process of releasing one of the carbon in the form of CO and CO_2.

Improvement was taken further by addition of the amine group which overall exhibited higher liquid product conversion and hydrocarbon compounds than un-grafted catalysts. This study found that the WPO used in the hydrocracking process contained a lot of FFA and impurities. So that the hydrocracking process using LM without the addition of metal produces a relatively high amount oxygenates which is 29.3 wt.%. This indicates that LL is not selective enough to adsorb FFA. The addition of an amine group increases the selectivity of the liquid product and hydrocarbon compounds. For example, the yield of liquid products and the hydrocarbon compounds Ni-Pt-NH_2 catalysts increased by 79.3 wt.% and 55.9 wt.%, respectively. The amine group shifted the selectivity towards decarboxylation reaction where there is an interaction between the amine and carboxylate group which weakened the bond in the carbonyl group of FFA, leading to the scission of the C–C bond cleavage of the carboxyl group in FFA through decarboxylation. The reaction mostly occurred at terminal carbon, thus generating long chained molecules in the liquid fraction [26]. Furthermore, the oxygenate content in the liquid product of each grafted catalyst was significantly lower than that of the un-grafted catalyst. On the other hand, the coke formation was increased due to the blocking of the catalyst pore when the amine groups absorbed the WPO causing the molecules to be trapped in the catalyst pores.

3.3.1 Effect of temperature and catalyst: feed ratio in the catalytic activity of WPO using NiPt-NH_2-LM

In this study, the catalyst that has the best catalytic activity and selectivity is NiPt-NH_2/LM. Hereinafter, the NiPt-NH_2/LM catalyst will be subjected to variations in temperature and catalyst: feed ratio in the process of converting WPO into biofuel. As can be seen in Table 4, the highest conversion of liquid product was produced at a temperature of 550 ^oC. A significant increase in liquid products and hydrocarbon compounds occurred from a temperature of 500 ^oC to 550 ^oC. This was probably caused by the amount of WPO that was adsorbed into liquid products in proportion to the amount of carbon compounds produced [49]. At a temperature of 600 ^oC, the activity and selectivity of the catalyst decreased due to the incomplete cracking process, resulting in the thermal decomposition. This thermal decomposition causes the cracking of long hydrocarbons into lighter hydrocarbons [50,51]. Besides that, it also increases the formation of gases supporting the formation coke.

Coke formation decrease with increasing temperature. This proves that with an increase in temperature, the feed can be well adsorbed and produce high liquid products and hydro-

Copyright © 2022, ISSN 1978-2993

carbon compounds. However, at a temperature of 600 °C coke increases. This is because WPO can not be absorbed into liquid products and deposited on the surface of the catalyst [52].

The decrease in product gas from a temperature of 500 °C to 550 °C is caused by perfect cracking, so that WPO can be converted into gasoline and diesel. But a temperature of 600 °C there is an increase in gas product cause by cracking that occur at high temperatures. So this can be attributed to the fact that higher temperature accelerated thermal decomposition, thereby breaking long-chain hydrocarbons into light hydrocarbons molecule [53].

Table 4 shows that the best temperature also affects the activity and selectivity of the WPO hydrocracking process. The higher the temperature, the liquid product and hydrocarbon compounds decrease. Moreover, the lower the temperature, the lower the liquid product and hydrocarbon compounds. With the result that, the optimum temperature is needed in the WPO cracking process to obtain liquid products and high hydrocarbon compounds [54,55]. At the optimum temperature (550 °C) obtained liquid products and hydrocarbon compounds of 79.3 wt.% and 55.9 wt.%, respectively.

After obtaining the best NiPt-NH_2/LM catalyst activity and selectivity at a temperature of 550 °C, the next step is to vary the catalyst: feed ratio. The ratio catalyst: feed used is 1:50, 1:100, and 1:200 (w/w). In the fact that increasing the catalyst: feed ratio leads to decrease in the liquid product and hydrocarbon compounds. This is possible because the greater the catalyst: feed ratio, the greater the amount of feed that interacts with the catalyst surface. The greater the interaction between the catalyst: feed ratio causes the formation of coke which blocks the pores of the catalyst, causing prevents the cracking process [56].

Table 4 indicates an increase in gas products. This is probably due to the occurrence of decarboxylation / decarbonylation mechanism. This mechanism removes one carbon from the ester chain in the form of carbon dioxide and the reduction stops in the production of aldehydes/ ketones [57]. There is decrease in organic compounds along with an increase in the ratio of catalyst:feed. This is because the liquid product contains more hydrocarbon compounds than other organic compounds (Table 4).

3.3.2 Reusability of NiPt-NH_2/LM catalyst in hydrocracking of WPO

NiPt-NH_2/LM catalyst was the best catalyst with a temperature and catalyst:feed ratio of 550 °C and 1:50, respectively. Furthermore, the reusability of the NiPt-NH_2/LM catalyst was carried out for 3 runs to test the stability of the catalyst in the WPO hydrocracking process. As shown in Table 5, there was decrease in the liquid product and hydrocarbon compounds, after the reusability. The distribution of the liquid products ($C_5 - C_{12}$ and $C_{13} - C_{20}$) decrease with reuse of the catalyst and cause an increase in the gaseous product.

The decrease in the activity and selectivity of the catalyst was caused by the formation coke which blocks the pores of the catalyst and covers the active site of the catalyst, thereby inhibiting the catalytic process. Some of the things that cause the deactivation of the catalyst are poisoning and coke formation. Poisoning is often caused by the chemisorption of impurities on the catalyst, whereas coke result from the formation and deposition of carbon on the catalyst. Carbon can be formed as a product or an intermediate resulting from side reaction, in both cases blocking the active site. Both coke formation a poisoning by heavy met-

Table 4. Product conversion and liquid product fraction using NiPt-NH_2-LM catalyst under temperature and catalyst:feed ratio variation

Hydrocracking conditions	Total Conversion (wt.%)	Product distribution (wt.%)						
		Gas Product	Liquid Product					Coke
			C_5-C_{12}	C_{13}-C_{20}	Total hydrocarbons	Oxygenates	Others	
Variations of temperature with catalyst:feed of 1:50								
500 °C	99.8	59.4	22.8	8.8	10.9	2.1	5.7	1.0
550 °C	99.7	20.4	27.4	28.5	55.9	6.8	16.6	0.3
600 °C	99.8	40.0	19.5	33.2	52.7	2.8	3.8	0.5
Variations of catalyst:feed ratio with temperature of 550 °C								
1:100	99.8	41.5	24.5	25.2	49.7	3.2	16.6	0.6
1:200	99.8	67.4	9.4	13.1	22.5	5.3	5.6	0.2

*Coke is waste palm oil that is deposited on the surface of the catalyst which cannot be converted into biofuel

Copyright © 2022, ISSN 1978-2993

als lead to deactivation of the catalyst during cracking which may or may not be reserved [58-60]. Table 5 points out that the product gas increases due to deactivation catalyst. Deactivation of the catalyst causes localized and uncontrolled cracking process [61]. A decrease in activity catalyst followed by a decrease in selectivity, but it can be seen that the reusability of the catalyst is able to reduce the oxygenate compound.

Figure 6 shows the morphology of the NiPt-NH_2/LM catalyst before and after the hydrocracking process. Before the hydrocracking process, the material did not show agglomeration. However, after hydrocracking process occurs agglomeration and form of dark spot. Dark spot could be spotted on the catalyst which was expected from the formation of coke causing pore blockage, therefore inhibited the interaction between catalyst and feed.

4. Conclusion

Catalytic hydrocracking of waste palm oil (WPO) was carried out using a catalyst made from the raw material of Lapindo mud (LM) which was modified using Ni and Pt metals as well as grafting using NH_2. The use of bimetallic metal catalysts is more promising in the hydrocracking process. The presence bimetallic metal can increase the activity and selectivity in the hydrocracking process. In addition, the amine group grafting process can reduce the oxygenate compounds produced in the liquid product. In this study, NiPt-NH_2/LM was the best catalyst in the hydrocracking process at a temperature of 550 °C and a catalyst: feed ratio 1:50. The liquid products and hydrocarbon compounds produced by the NiPt-NH_2/LM catalyst were 79.4 wt.% and 55.9 wt.%, respectively. A reusability test was also done on the NiPt-NH_2/LM catalyst and the results indicated that the liquid product and hydrocarbon compounds decreased after the reusability test catalyst. However, the liquid product produced after the use of the second and third catalyst still showed the presence hydrocarbon compounds. The amount of hydrocarbon compounds produced after the third reusability test was 23.6 wt.%. In overall, the metal-based and amine-functionalized catalysts significantly improved the catalytic activity and selectivity towards liquid products and hydrocarbon compounds by reducing oxygenated compound.

Table 5. Product conversion and liquid fraction using NiPt-NH_2-LM catalyst in reusability test

Hydrocracking conditions	Total Conversion (wt.%)	Product distribution (wt.%)						
		Gas Product	Liquid Product					Coke
			C_5-C_{12}	C_{13}-C_{20}	Total hydrocarbons	Oxygenates	Others	
NiPt-NH_2/LM[1]	99.7	20.4	27.4	28.5	55.9	6.8	16.6	0.3
NiPt-NH_2/LM[2]	99.7	84.2	4.0	5.9	9.9	2.2	1.8	1.6
NiPt-NH_2/LM[3]	99.8	71.2	12.9	10.7	23.6	1.6	3.2	0.2

[1]The first hydrocracking used a NiPt-NH_2/LM catalyst.
[2]The second hydrocracking used a NiPt-NH_2/LM catalyst.
[3]The third hydrocracking used a NiPt-NH_2/LM catalyst.

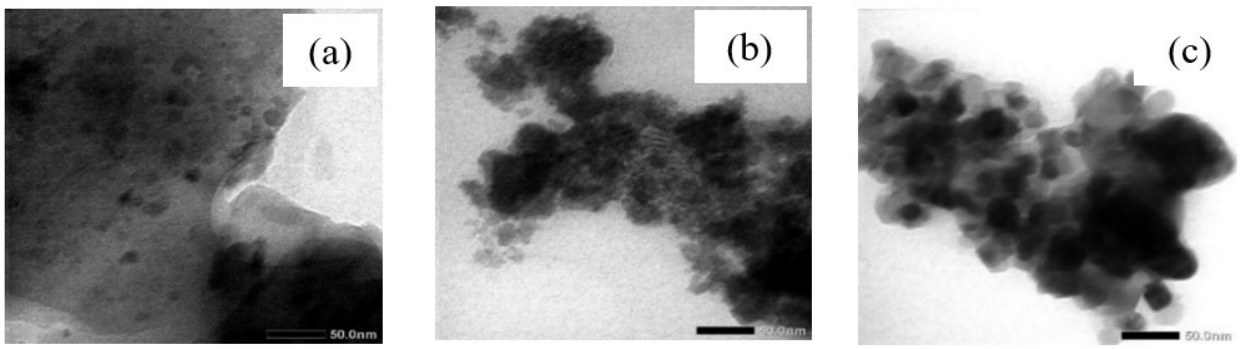

Figure 6. TEM images of NiPt-NH_2/LL (a) fresh (b) after one-time hydrocracking (c) after second-time hydrocracking

Copyright © 2022, ISSN 1978-2993

Acknowledgement

The authors would like to thank the Ministry of Research, Technology, and Higher Education of Indonesia for the financial support under the scheme of PTUPT research grant 2021 (Contact number: 2127/UN1/DITLIT/DITLIT/PT/2021).

References

[1] Plazas-González, M,. Guerrero-Fajardo C.A., Sodré J.R. (2018). Modelling and simulation of hydrotreating of palm oil components to obtain green diesel. *Journal of Cleaner Production*, 184, 301-308. DOI: 10.1016/j.jclepro.2018.02.275

[2] Del Río, J.I., Cardeno, F., Pérez, W., Pena, J.D., Rios, L.A. (2018). Catalytic hydrotreating of jatropha oil into non-isomerized renewable diesel: Effect of catalyst type and process conditions, *Chemical Engineering Journal*, 352, 232-240. DOI: 10.1016/j.cej.2018.07.021

[3] Taufiqurahmi, N., Mohamed, A.R., Bhatia, S. (2011). Production of biofuel from waste cooking palm oil using nanocrystalline zeolite as catalyst: Process optimization studies, *Bioresource Technology*, 102, 10686-10694. DOI: 10.1016/j.biortech.2011.08.068

[4] Dinesha, P., Kumar, S., Rosen, M.A. (2019). Performance and emission analysis of a domestic wick stove using biofuel feedstock derived from waste cooking oil and sesame oil. *Renewable Energy*, 136, 342-351. DOI: 10.1016/j.renene.2018.12.118

[5] Liu, T., Liu, Y., Wu, S., Xue, J., Wu, Y., Li, Y., Kang, X. (2018). Restaurant's behaviour, awareness, and willingness to submit waste cooking oil for biofuel production in Beijing. *Journal of Cleaner Production*, 204, 636-642. DOI: 1016/j.jcepro.2018.09.056

[6] Yang, H., Chien, S., Lo, M., Lan, J.C., Lu, W., Ku, Y. (2007). Effects of biodiesel on emissions of regulated air pollutants and polycyclic aromatic hydrocarbons under engine durability testing. *Atmospheric Environment*, 41, 7232-7240. DOI: 10.1016/j.atmosenv.2007.05.019

[7] Wang, Y., Cao, Y., Li, J. (2018). Preparation of biofuels with waste cooking oil by fluid catalytic cracking: The effect of catalyst performances on products. *Renewable Energy,* 124, 34-39. DOI: 10.1016/j.renene.2017.08.084

[8] Zhang, H., Lin, H., Wang, W., Zheng, Y., Hu, P. (2014). Hydroprocessing of waste cooking oil over a dispersed nano catalyst: Kinetics study and temperature effect. *Applied Catalysis B: Environmental*, 150-151, 238-248. DOI: 10.1016/j.apcatb.2013.12.006

[9] Mahdi, H.I., Bazargan, A., McKay, G., Azelee, N.I.W., Meili, L. (2021). Catalytic deoxygenation of palm oil and its residue in green diesel production: A current technological review. *Chemical Engineering Research and Design*, 174, 158-187. DOI: 10.1016/j.cherd.2021.07.009

[10] Khodadi, M.R., Malpartida, I., Tsang, C., Lin, C.S.K., Len, C. (2020). Recent advances on the catalytic conversion of waste cooking oil. *Molecular Catalysis*, 494, 111128. DOI: 10.1016/j.mcat.2020.111128

[11] Mironenko, O.O., Sosnin, G.A., Eletskii, P.M., Gulyaeva, Y.K., Bulavchenko, O.A., Stonkus, O.A., Rodina, V.O., Yakovlev, V.A. (2017). A study of the catalytic steam cracking of heavy crude oil in the presence of a disperses molybdenum-containing catalyst. *Petroleum Chemistry*, 57(7), 618-629. DOI: 10.1134/S0965544117070088

[12] Pham, D.V., Nguyen, N.T., Kang, K.H,. Seo, P.W., Kim, G.T., Park, Y., Park, S. (2022). Effect of slurry phase catalyst and H_2 pressure on hydrocracking of SDA (solvent deasphalting) pitch. *Korean Journal of Chemical Engineering*, 39, 1215-1226. DOI: 10.1007/s11814-021-1026-7

[13] Regali, F., París, R.S., Aho, A., Boutonnet, M., Järås, S. (2013). Deactivation of Pt/silica-alumina and effect on selectivity in the hydrocracking of n-hexadecane. *Topics in Catalysis*, 56, 594-601. DOI: 10.1007/s11244-013-0011-8

[14] Doronin, V.P., Sorokina, T.P., Potapenko, O.V. (2019). The formation of properties of ultrastable zeolite Y for cracking and hydrocracking catalysts. *Petroleum Chemistry*, 59(3), 310-317. DOI: 10.1134/S0965544119030046

[15] Maximov, N.M., Zurnina, A.A., Dokuchaev, I.S., Solmanov, P.S., Eremina, Y.V., Zhilkina, E.O., Koptenatmusov, V.B., Pimerzin, A.A. (2021). Comparative analysis of transformations of heavy oil feedstock model components under cracking conditions in the presence of metal and acid catalysts. *Chemistry Technology of Fuels and Oil*, 56(6), 878-884. DOI: 10.107/s10553-021-01203-4

[16] Thangadurai, T., Tye, C.T. (2021) Acidity and basicity of metal oxide-based catalysts in catalytic cracking of vegetable oil. *Brazilian Journal of Chemical and Engineering*, 38, 1-20. DOI: 10.1007/s43153-020-0085-z

[17] De, S., Zhang, J., Luque, R., Yan, N. (2016) Ni-based bimetallic heterogeneous catalysts for energy and environmental applications. *Energy and Environmental Sciences*, 9, 3314-3347. DOI: 10.1039/C6EE02002J

Copyright © 2022, ISSN 1978-2993

[18] Mayorga, M.A., Cadavid, J.G., Palacios, O.Y.S., Vargas, J., González, J., Narváez, P.C. (2019). Production of renewable diesel by hydrotreating of palm oil with noble metallic catalysts. *Chemical Engineering Transaction*, 74, 7-12. DOI: 10.3303/CET1974002

[19] Talib, N.B., Triwahyono, S., Jalil, A., Mamat, C.R., Salamun, N., Fatah, N.A.A., Sidik, S.M., The, L.P. (2016). Utilization of a cost effective Lapindo mud catalyst derived from eruption waste for transesterification of waste oils. *Energy Conversion and Management*, 108, 411-421. DOI: 10.1016/j.enconman.2015.11.031

[20] Puspitasari, R.N., Budiarti, H.A., Hatta, A.M., Sekartedjo, Risanti, D.D. (2017). Enhanced dye-sensitized solar cells performance through novel core-shell structure of gold nanoparticles and nano-silica extracted from Lapindo mud. *Procedia Engineering*, 170, 93-100. DOI: 10.1016/j.proeng.2017.03.018

[21] Valenstein, J.S., Kandel, K., Melcher, F., Slowing, I.I., Lin, V.S., Trewyn, B.G. (2017). Functional mesoporous silica nanoparticles for the selective sequestration of free fatty acids from microalgal oil. *ACS Applied Material & Interfaces*, 4, 1003-1009. DOI: 10.1021/am201647t

[22] Kandel, K., Frederickson, C., Smith, E.A., Lee, Y., Slowing, I.I, (2013) Bifunctional adsorbent-catalytic nanoparticles for the refining of renewable feedstocks. *ACS Catalysis*, 3, 2750-2758. DOI: 10.1021/cs4008039

[23] Kord, M., Nematollahzadeh, A., Mirzayi, B. (2019). Second-order isothermal reaction in a semi-batch reactor: modeling, exact analytical solution, and experimental verification. *Reaction Chemistry & Engineering*, 4, 2011-2020. DOI: https://doi.org/10.1039/C9RE00174C

[24] Kim, H., Nguyen-Huy, C., Shin, E.W. (2014). Macroporous NiMo/alumina catalyst for the hydrocracking of vacuum residue. *Reaction Kinetics, Mechanism and Catalysis*, 113, 431-443. DOI: 10.1007/s11144-014-0764-5

[25] Ting-ting, W,. Yang, L., Li-jun. J., De-chao, W., De-meng, Y., Hao-quan, H. (2019). Upgrading of coal tar with steam catalytic cracking over Al/Ce and Al/Zr co-doped Fe_2O_3 catalysts. *Journal of Fuel Chemistry and Technology*, 47(3), 287-296. DOI: 10.1016/S1872-5813(19)30013-1

[26] Trisunaryanti, W., Larasati, S., Bahri, S., Ni'mah,Y.L., Efiyanti, L., Amri, K., Nuryanto, R., Sumbogo, S.D, (2020). Performance comparison of Ni-Fe loaded on NH_2-functionalized mesoporous silica and beach sand in hydrotreatment of waste palm cooking oil. *Journal of Environmental Chemical Engineering*, 8, 104477. DOI: 10.1016/j.jece.2020.104477

[27] Ebrahiminejad, M., Karimzadeh, R. (2022). Diesel hydrocracking and hydrodesulfurization with activated red mud-supported and fluorine-containing NiW nanocatalysts. *Molecular Catalysis*, 517, 112056. DOI: 10.1016/j.mcat.2021.112056

[28] Ge, Y., Jia, Z., Gao, C., Gao, P., Zhao, L., Zhao, Y. (2014). Synthesis of mesoporous silica-alumina materials via urea-templated sol-gel route and their catalytic performance for THF polymerization. *Russian Journal Physical Chemistry*, 88, 1650-1655. DOI: 10.1134/S0036024414100355

[29] Aneu, A., Wijaya, K., Syoufian, A. (2021). Silica-based acid catalyst with different concentration H_2SO_4 and calcination temperature: Preparation and characterization. *Silicon*, 13, 2265-22670. DOI: 10.1007/s12633-020-00741-6

[30] Kusumastuti, H., Trisunaryanti, W., Falah, I.I., Marsuki, M.F. (2018) Synthesis of mesoporous silica-alumina from Lapindo mud as a support of Ni and Mo metals catalysts for hydrocracking of pyrolyzed α-celulose. *RASĀYAN Journal of Chemistry*, 11(2), 522-530. DOI: 10.7324/RJC.2018.1122061

[31] Tanimu, A., Jillani, S.M.S., Ganiyu, S.A., Chowdhury, S., Alhooshani, K. (2021). Multivariate optimization of chlorinated hydrocarbons' micro-solid-phase extraction from wastewater using germania decorated mesoporous alumina-silica sorbent and analysis by GC-MS. *Microchemical Journal*, 160, 105674. DOI: 10.1016/j.microc.2020.105674

[32] Tran, T.H.Y., Schut, H., Haije, W.G., Schoonman, J. (2011). Structural characterization and porosity analysis in self-supported porous alumina-silica thin films. *Thin Solid Films*, 520, 30-34. DOI: 10.1016/j.tsf.2011.06.027

[33] Mardkhe, M.K., Huang, B., Bartholomew, C.H., Alam, T.M., Woodfield, B.F. (2016). Synthesis and characterization of silica doped alumina catalyst support with superior thermal stability and unique pore properties. *Journal of Porous Materials*, 23, 475-487. DOI: 10.1007/s10934-015-0101-z

[34] Kumar, M.S., Vanmathi, M., Senguttuvan, G., Mangalaraja, R.V., Sakthivel, G. (2019). Fly ash constituent-silica and alumina role in the synthesis and characterization of cordierite based ceramics. *Silicon*, 11, 2599-2611. DOI: 10.1007/s12633-018-0049-0

[35] Molero, H., Galarraga, C., Geng, F., Hernandez, E., Birss, V., Pereira, P. (2009) High performance Ni based catalyst for toluene hydrocracking. *Catalysis Letters*, 132, 402-409. DOI: 10.1007/s10562-009-0128-3

Copyright © 2022, ISSN 1978-2993

[36] Chumachenko, V.A., Lavrenov, A.V., Buluchevskii, E.A., Arbuzov, A.B., Gulyaeva, T.I., Drozdov, V.A. (2016). Hydrocracking of vegetable oil on boron-containing catalysts: Effect of the nature and content of a hydrogenation component. *Catalysis in Industry*, 8, 56-74. DOI: 10.1134/S2070050416010037

[37] Kostyniuk, A., Bajec, D., Likozar, B. (2021). Catalytic hydrogenation, hydrocracking and isomerization reaction of biomass tar model compound mixture over Ni-modified zeolite catalysts in packed bed reactor. *Renewable Energy*, 167, 409-424. DOI: 10.1016/j.renene.2020.11.098

[38] Bozorgi, B., Karimi-Sabet, J., Khadiv-Parsi, P. (2022). The removal of N_2O from gas stream by catalytic decomposition over Pt-alkali metal/SiO_2. *Environmental Technology and Innovation*, 26, 102344. DOI: 10.1016/j.eti.2022.102344

[39] Dubey, R.S., Rajesh, Y.B.R.D., More, M.A. (2015) Synthesis and characterization of SiO_2 nanoparticles via sol-gel method for industrial applications. *Materials Today: Proceedings*, 2(4-5), 3575-3579. DOI: 10.1016/j.matpr.2015.07.098

[40] Li-wei, Z., Jian-gang, W., Ping-ping, Z., Feng, S., Xiu-yiu, S., Lihong, W., Hong-you, C., Weiming, Y. (2017). Preparation of the Nb-P/SBA-15 catalyst and its performance in the dehydration of fructose to 5-hydroxymethylfurfural. *Journal of Fuel Chemistry and Technology*, 45(6), 651-659. DOI: 10.1016/S1872-5813(17)30034-8

[41] Francis, J., Guillon, E., Bats, N., Pichon, C., Corma, A., Simon, L.J. (2011). design of improved hydrocracking catalysts by increasing the proximity between acid and metallic sites. *Applied Catalysis A: General*, 409-410, 140-147. DOI: 10.1016/j.apcata.2011.09.040

[42] Pratiwi, R.G., Wantala, K. (2022). Hydroconversion of palm oil via continuously pyrolytic catalysis to biofuels over oxide-based catalyst derived from waste blood clamshell: Effect of magnesium contents. *Molecular Catalysis*, 523, 111468. DOI: 10.1016/j.mcat.2021.111468

[43] Alisha, G.D., Trisunaryanti, W., Syoufian, A. (2022). Mesoporous silica from Parangtritis beach sand templated by CTAB as a support of Mo metal as a catalyst for hydrocracking of waste palm cooking oil into biofuel. *Waste and Biomass Valorization*, 13, 1311-1321. DOI: 10.1007/s12649-021-01559-y

[44] Ma, Y., Liang, R., Wu, W., Zhang, J., Cao, Y., Huang, K., Jiang, L. (2021). Enhancing the activity of MoS_2/SiO_2-Al_2O_3 bifunctional catalysts for suspended-bed hydrocracking of heavy oils by doping with Zr atoms. *Chinese Journal of Chemical Engineering*, 39, 126-134 (2021). DOI: 10.1016/j.cjche.2021.03.015

[45] Subsadsana, M., Kham-or, P., Sangdara, P., Suwannasom, P., Ruangviriyachai, C. (2017). Synthesis and catalytic performance of bimetallic NiMO- and NiW-ZSM-5/MCM-41 composites for production of liquid biofuels. *Journal of Fuel Chemistry and Technology*, 45(7), 805-816. DOI: 10.1016/S1872-5813(17)30039-7

[46] Do, P.T.M., Foster, A.J., Chen, J., Lobo, R.F. (2012). Bimetallic effects in the hydrodeoxygenation of meta-cresol on γAl_2O_3 supported Pt-Ni and Pt-Co catalysts. *Green Chemistry*, 14, 1388-1397. DOI: 10.1039/C2GC16544A

[47] Žula, M., Grilc, M., Likozar, B. (2022). Hydrocracking hydrogenation and hydrodeoxygenation of fatty acids, esters and glycerides: Mechanisms, kinetics, and transport phenomena. *Chemical Engineering Journal*, 444, 136564. DOI: 10.1016.j.cej.2022.136564

[48] Kang, J., Ma, W., Keogh, R.A., Shafer, W.D., Jacobs, G., Davis, B.H. (2012). Hydrocracking and hydroisomerization of n-Hexadecane, n-Octacosane and Fischer-Tropsch wax over a Pt/SiO_2-Al_2O_3 Catalyst. *Catalysis Letters*, 142, 1295-1305. DOI: 10.10117/s10562-012-0910-5

[49] Wang, H., Farooqi, H., Chen, J. (2015). Co-hydrotreating light cycle oil-canola oil blends. *Frontiers of Chemical Science and Engineering*, 9(1), 64-76. DOI: 10.1007/s11705-015-1504-8

[50] Trieu, T.Q., Guan, G., Liu, G., Tsubaki, N., Samart, C., Reubroycharoen, P. (2017). Direct synthesis of iso-paraffin fuel from palm oil on mixed heterogeneous acid and base catalysts. *Montash für Chemies*, 148, 1235-1243. DOI: 10.1007/s00706-017-1963-3

[51] Lovás, P., Hudec, P., Hadvinová, M., Ház, A. (2015). Use of ZSM-5 catalyst in deoxygenation of waste cooking oil. *Chemical Papers*, 69(11), 1454-1464. DOI: 10.1515/chempap-2015-0159

[52] Tóth, C., Sági, D., Hancsók, J. (2015). Diesel fuel production by catalytic hydrogenation of light cycle oil and waste cooking oil containing gas oil. *Topics in Catalysis*, 58, 948-960. DOI: 10.1007/s11244-015-0463-0

[53] Ahmadi, S., Yuan, Z., Rohani, S., Xu, C. (2015). Effects of nano-structured CoMo catalysts on hydrodeoxygenation of fast pyrolysis oil in supercritical ethanol. *Catalysis Today*, 269, 182-194. DOI: 10.1016/j.cattod.2015.08.040

Copyright © 2022, ISSN 1978-2993

[54] Wijaya, K., Kurniawan, M.A., Saputri, W.D., Trisunaryanti, W., Mirzan, M., Hariani, P.L., Tikoalu, A.D. (2021). Synthesis of nickel catalyst supported on ZrO_2/SO_4 pillared bentonite and its application for conversion of coconut oil into gasoline via hydrocracking process. *Journal of Environmental Chemical Engineering*, 9, 105399. DOI: 10.1016/j.jece.2021.105399

[55] Pongsendana, M., Trisunaryanti, W., Artanti, F.W., Falah, I.I., Sutarno. (2017), Hydrocracking of waste lubricant into gasoline fraction over CoMo catalyst supported on mesoporous carbon from bovine bone gelatin. *Korean Journal of Chemical Engineering*, 34, 2591-2596. DOI: 10.1007/s11814-017-0165-3

[56] Chen, J., Shi, H., Li, L., Li, K. (2014). Deoxygenation of methyl laurate as a model compound to hydrocarbons on transition metal phosphide catalysts. *Applied Catalysis B : Environmental*, 144. 870-884. DOI: 10.1016/j.apcatb.2013.08.026

[57] Saab, R., Polychronopoulou, K., Zheng, L., Kumar, S., Schiffer, A. (2020). Synthesis and performance evaluation of hydrocracking catalysts: A review. *Journal of Industrial and Engineering Chemistry*, 89, 83-103. DOI: 10.1016/j.jiec.2020.06.022

[58] Landa, L., Remiro, A., Valecillos, J., Valle, B., Bilbao, J., Gayubo, A.G. (2022). Unveiling the deactivation by coke of $NiAl_2O_4$ spinel derived catalysts in the bio-oil steam reforming: Role of individual oxygenates. *Fuel*, 321, 124009. DOI: 10.1016/j.fuel.2022.124009

[59] He, S., Goldhorn, H.R., Tegudeer, Z., Chandel, A., Heeres, A., Stuart, M.C.A., Heeres, H.J. (2022). A time- and space resolved catalyst deactivation study on the conversion of glycerol to aromatics using H-ZSM-5. *Chemical Engineering Journal*, 434, 134620. DOI: 10.1016/j.cej.2022.134620

[60] He, S., Klei, F.G.H., Kramer, T.S., Chandel, A., Tegudeer, Z., Heeres, A., Heeres, H.J. (2022). Catalytic co-conversion of glycerol and oleic acid to bio-aromatics: catalyst deactivation studies for a technical H-ZSM-5/Al_2O_3 catalyst. *Applied Catalysis A : General*, 632, 118486. DOI: 10.1016/j.apcata.2022.118486

Copyright © 2022, ISSN 1978-2993